

Three-Electrode Electrochemical Detector and Platinum Film Decoupler Integrated with a Capillary Electrophoresis Microchip for Amperometric Detection

Ching-Chou Wu,[†] Ren-Guei Wu,[†] Jenn-Gunn Huang,[†] Yu-Cheng Lin,[‡] and Hsien-Chang Chang^{*,†}

Institute of Biomedical Engineering and Institute of Engineering Science, National Cheng Kung University,
No. 1 Ta-Hseuh Road, Tainan, Taiwan 70101

This article demonstrates that a three-electrode electrochemical (EC) detector and an electric decoupler could be fabricated in the same glass chip and integrated with an O₂-plasma-treated PDMS layer using microfabrication techniques to form the capillary electrophoresis (CE) microchip. The platinized decoupler could mostly decouple the electrochemical detection circuit from the interference of an separation electric field in 10 mM 2-(N-morpholino)ethanesulfonic acid (MES, pH 6.5) solution. The baseline offset of background current recorded from the working electrode with and without application of a separation electric field was maintained at less than 0.05 pA in 10 mM MES. In addition, the platinized pseudoreference electrode was demonstrated to offer a stable potential in electrochemical detection. As a consequence, the limit of detection of dopamine was 0.125 μ M at a S/N = 4. The responses for dopamine to different concentrations were found to be linear between 0.25 and 50 μ M with a correlation coefficient of 0.9974 and a sensitivity of 11.76 pA/ μ M. The totally integrated CE-EC microchip should be able to fulfill the ideal of miniaturization and commercialization.

The high separation efficiency of capillary electrophoresis (CE) has attracted considerably widespread interest in the separation technique field. The most popular detection modes equipped in commercial CE instruments are UV/visible absorbance and fluorescence. With the features of broad applicability and easy direct measurement without any external chemical derivatization, absorbance detection is considerably suitable for mass routine analysis. Owing to the short optical path length depending upon capillary diameter, the detection limit typically ranges from 10⁻⁵ to 10⁻⁷ M.^{1,2} Although there have been reports to describe some methods that could possibly lower the detection limit,^{2,3} the detection limit of UV/visible absorbance is still higher than that

of fluorescence. Laser-induced fluorescence (LIF) detection can offer high sensitivity, but it generally requires a derivatization of the analytes. Also expensive, bulky, and complicated instrumentation was required for LIF detection. Recently, it is available to miniaturize and integrate LIF detection with a CE microchip to form a compact system by using the microfabrication technique.^{4,5}

In addition to the optical detectors, electrochemistry (EC) detectors seem to be another excellent option for CE measurement raised from the advantages of relatively low cost, high sensitivity, and excellent suitability for miniaturization. EC detection has already proven to be widely employed in conventional CE systems to detect compounds possessing electrochemical activity. The use of CE-EC was first reported by Wallingford and Ewing in 1987,⁶ but commercialization of EC detectors has been limited by a number of problems; for example, the interference of a high separation electric field can affect the stability of the EC background current, and the position of working electrodes from the outlet of the CE column can affect the reproducibility of EC measurement.^{7–9} Most EC installation in CE detection is referred to as end-column detection, in which the working electrode is positioned at the end of the capillary. Usually the EC detection current and the shift of half-wave potential of analytes are affected by the position of the working electrode which is relative to the capillary outlet.⁷ A precise stereopositioner is required to align the fragile working electrode into the separation column. For solving the problem of using the positioner, Wang et al. presented methods of not using an extra positioner by means of the combination of microphotolithographically fabricated separation chips and thick-film electrochemical detectors.^{10,11} Furthermore, in Chen's study, the working electrode was directly

* Corresponding author. E-mail: hcchang@mail.ncku.edu.tw. Fax: 886-6-276-0697.

[†] Institute of Biomedical Engineering.

[‡] Institute of Engineering Science.

(1) Qurishi, R.; Kaulich, M.; Muller, C. E. *J. Chromatogr., A* **2002**, *952*, 275–281.

(2) Culbertson, C. T.; Jorgenson, J. W. *Anal. Chem.* **1998**, *70*, 2629–2638.

(3) Moring, S. E.; Reel, R. T. *Anal. Chem.* **1993**, *65*, 3454–3459.

(4) Burns, M. A.; Johnson, B. N.; Brahmasandra, S. N.; Handique, K.; Webster, J. R.; Krishnan, M.; Sammarco, T. S.; Man, P. M.; Jones, D.; Heldsinger, D.; Mastrangelo, C. H.; Burke, D. T. *Science* **1998**, *282*, 484–487.

(5) Chabinyk, M. L.; Chiu, D. T.; McDonald, C.; Stroock, A. D.; Christian, J. F.; Karger, A. M.; Whitesides, G. M. *Anal. Chem.* **2001**, *73*, 4491–4498.

(6) Wallingford, R. A.; Ewing, A. G. *Anal. Chem.* **1987**, *59*, 1762–1766.

(7) Wallenborg, S. R.; Nyholm, L.; Lunte, C. E. *Anal. Chem.* **1999**, *71*, 544–549.

(8) Park, S.; McGrath, M. J.; Smyth, M. R.; Diamond, D.; Lunte, C. *Anal. Chem.* **1997**, *69*, 2994–3001.

(9) Matysik, F. M. *J. Chromatogr., A* **1996**, *742*, 229–234.

(10) Wang, J.; Tian, B.; Sahlin, E. *Anal. Chem.* **1999**, *71*, 5436–5440.

(11) Wang, J.; Tian, B.; Sahlin, E. *Anal. Chem.* **1999**, *71*, 3901–3904.

integrated on the CE microchip to improve the reproducibility of channel–electrode alignment and spacing.¹²

Another concern in CE with EC detection is the interference of high electric field and electrophoretic current on EC measurement. The interference results in a larger EC background current and a shifted redox potential.^{7,9} To eliminate the interference raised from the high electric field and to protect the EC detector from the damage of surge spikes, a decoupler placed prior to the working electrode was used to separate the EC detection system from the interference of CE circuitry. Currently, several kinds of decouplers were fabricated: such as a porous glass joint,⁶ porous graphite tubing,¹³ etched capillary,¹⁴ polymeric materials,^{15,16} or Pd solid-state metal.¹⁷ The fabrication of a joint-connected decoupler device in a CE-EC system is inconvenient and not easily implemented due to the features of fragility, leakage of analytes, and dead volume. The dead volume is defined as the non-EOF-driven space between the decoupler and working electrode. The dead volume could cause lower detection peak current. Wallenborg et al. reported that the distance between the end of the capillary and the detection electrode should be as short as possible for minimizing the diffusional and convective broadening of the analyte zone.⁷ Similarly, Chen addressed the situation where the closer the distance between decoupler and working electrode was set, the larger the amperometric current that could be obtained. Furthermore, to solve the problems of fragility and leakage of analytes, Chen et al. developed a Pd solid film integrated directly into the CE microchip across the separation channel by micro-fabrication techniques which was served instead of the decoupler of joint connection type.¹² The rationale to adopt the Pd metal is that the platinum group metals such as Pd and Pt could effectively reduce and absorb hydrogen ion. So hydrogen could diffuse faster on a Pd surface. Therefore, hydrogen is removed from the Pd decoupler before the formation of hydrogen bubbles for the EOF maintains the decoupling efficiency of the decoupler.^{12,17} An alternative approach that could decrease the effect of the CE field on EC detection instead of decouplers is to utilize a narrower inner diameter capillary (<25 μm).¹⁵ Nevertheless, the smaller inner diameter column is easily obstructed by gas bubbles or impurities.

The “lab-on-a-chip” design could possibly supply the answer to solve the above problems. The advantages of a microchip include lower consumption of solvent and reagent, shorter analysis time, portability, and disposability. A CE microchip with electrochemical detection can be briefly divided into two concerns. One part is the fabrication of the CE separation channel. It is necessary to supply the strength of EOF in the separation channel of a microchip. In general, most CE microchips have been constructed from glass or quartz because such materials were suitable for optical detection and easily allowed EOF, but fabrication of a glass substrate microchip required a crucial clean room and highly thermal bonding ($\sim 600^\circ\text{C}$) conditions, which were not easily

obtained in a general laboratory.^{18,19} Therefore, some alternative polymers, such as poly(methyl methacrylate), polycarbonate, polyethylene, and poly(dimethylsiloxane) (PDMS), were adopted to form the CE microfluidic channel instead of glass or silicon.²⁰ Among these polymers, PDMS has been widely discussed due to several characteristics: (i) optical transparency down to 230 nm is suitable for optical detection; (ii) it cures at low temperatures and molding can easily be replicated through the process of prototyping, master formation, and soft lithography; (iii) it can seal reversibly to itself and other materials by van der Waals contact with the clear smooth surface at room temperature; (iv) its surface chemistry can be controlled to form EOF using a plasma technique.^{21–23} The CE microchip that combined a PDMS slice with a glass substrate was first developed by Effenhauser.²⁴ Subsequently, many PDMS applications in CE chip and microfluidic channel design have been reported.^{25–27}

The other concern is the efficiency of EC detection. In general, three different kinds of electrochemical approaches (amperometry,^{10,11,28,29} conductimetry,^{30–33} voltammetry^{8,34}) have been used in CE detection. Amperometric detection is the most popular approach to quantify the redox reaction of analyte in CE application among these EC methods. However, the three-electrode EC detector has not been integrated with a CE system successfully until now. Although the decoupler device and working electrode are deposited on the same chip combined with the CE channel,¹² the reference electrode, of which most are Ag/AgCl, is usually inserted into the waste well located beyond the CE chip. Basically, the extra-added reference electrode is not really integrated into the CE-EC chip.

To be fully integrated into a CE-EC microchip, the three-electrode EC detector and decoupling device are deposited on the same glass substrate, which is sealed with a PDMS replica containing the injection and separation channels. Therefore, a very porous platinized electrode acting as decoupler was located in front of the three-electrode EC detector to isolate the interference from

- (12) Chen, D. C.; Hsu, F. L.; Zhan, D. Z.; Chen, C. H. *Anal. Chem.* **2001**, *73*, 758–762.
(13) Yik, Y. F.; Lee, H. K.; Li, S. F. Y.; Khoo, S. B. *J. Chromatogr.* **1991**, *585*, 139–144.
(14) Zhang, S. S.; Yuan, Z. B.; Liu, H. X.; Zou, H.; Wu, Y. J. *J. Chromatogr., A* **2000**, *872*, 259–268.
(15) Matsysik, F. M.; Meister, A.; Werner, G. *Anal. Chim. Acta* **1995**, *305*, 114–120.
(16) Zhou, J.; Lunte, S. M. *Anal. Chem.* **1995**, *67*, 13–18.
(17) Kok, W. T.; Sahin, Y. *Anal. Chem.* **1993**, *65*, 2497–2501.

- (18) Waters, L. C.; Jacobson, S. C.; Kroutchinina, N.; Khandurina, J.; Foote, R. S.; Ramsey, J. M. *Anal. Chem.* **1998**, *70*, 5172–5176.
(19) Kutter, J. P. *Trends Anal. Chem.* **2000**, *19*, 352–362.
(20) Becker, H.; Gärtner, C. *Electrophoresis* **2000**, *21*, 12–26.
(21) McDonald, J. C.; Duffy, D. C.; Anderson, J. R.; Chiu, D. T.; Wu, H.; Schueller, O. J. A.; Whitesides, G. M. *Electrophoresis* **2000**, *21*, 27–40.
(22) Ocvirk, G.; Munroe, M.; Tang, T.; Oleschuk, R.; Westra, K.; Harrison, D. J. *Electrophoresis* **2000**, *21*, 107–115.
(23) Deng, T.; Wu, H.; Brittain, S. T.; Whitesides, G. M. *Anal. Chem.* **2000**, *72*, 3176–3180.
(24) Effenhauser, C. S.; Bruin, G. J. M.; Paulus, A.; Ehrat, M. *Anal. Chem.* **1997**, *69*, 3451–3457.
(25) Martin, R. S.; Gawron, A. J.; Lunte, S. M.; Henry, C. S. *Anal. Chem.* **2000**, *72*, 3196–3202.
(26) Gawron, A. J.; Martin, R. S.; Lunte, S. M. *Electrophoresis* **2001**, *22*, 242–248.
(27) Duffy, D. C.; McDonald, J. C.; Schueller, O. J. A.; Whitesides, G. M. *Anal. Chem.* **1998**, *70*, 4974–4984.
(28) Woolley, A. T.; Lao, K.; Glazer, A. N.; Mathies, R. A. *Anal. Chem.* **1998**, *70*, 684–688.
(29) Wang, J.; Chatrathi, M. P.; Tian, B. *Anal. Chem.* **2000**, *72*, 5774–5778.
(30) Zemmann, A. J. *Trends Anal. Chem.* **2001**, *20*, 346–354.
(31) Gallagher, P. A.; Oertel, C. M.; Danielson, N. D. *J. Chromatogr., A* **1998**, *817*, 31–39.
(32) Tuma, P.; Opekar, F.; Jelinek, I.; Stulik, K. *Electroanalysis* **1999**, *11*, 1022–1026.
(33) Masar, M.; Zuborova, M.; Bielikova, J.; Kaniansky, D.; Johnck, M.; Stanislawski, B. *J. Chromatogr., A* **2001**, *916*, 101–111.
(34) Wang, J.; Polsky, R.; Tian, B.; Chatrathi, M. P. *Anal. Chem.* **2000**, *72*, 5285–5289.

CE voltage/current in this study. Moreover, a platinized electrode serving as the pseudoreference electrode was simultaneously integrated on the CE microchip and close to the working electrode in order to decrease the potential shift during amperometry detection. In this article, we demonstrate the performance efficiency of the integrated CE microchip with total EC detection electrodes and estimate the effects of a platinized decoupler and a platinized pseudoreference electrode on amperometric detection as a high voltage is applied for the CE separation.

EXPERIMENTAL SECTION

Reagent. The positive photoresists, S1818 and AZ PLP-40, and PDMS Sylgard 184 were purchased from Shipley Co., Clariant Co., and Dow Corning Corp., respectively. All other chemicals for chip cleaning and fabrication from J.T. Baker Corp., and all chemicals were used without any further purification. Chloroplatinic acid hexahydrate ($\text{H}_2\text{PtCl}_6 \cdot 6\text{H}_2\text{O}$) for depositing Pt on the Au electrode was purchased from Sigma. The running buffer was prepared from 10 mM 2-(*N*-morpholino)ethanesulfonic acid (MES, Sigma) titrated to pH 6.5 using 0.1 N NaOH and 10 mM phosphate buffer solution (PBS, pH 7.4, Sigma). The testing analytes included potassium ferrocyanide (Katayama), catechol (Sigma), and dopamine (Sigma), which were prepared fresh daily by serial dilution on the separation electrolyte.

Electrode Fabrication and Layout. All of the electrodes were fabricated by using standard photolithographic techniques, a wet chemical etching process,³⁵ and the glass slide used as a substrate was sequentially immersed in acetone and then a mixture medium of $\text{NH}_4\text{OH}/\text{H}_2\text{O}_2/\text{H}_2\text{O}$ (2:1:3) for cleaning before the deposition of the electrode. (**Caution!** The mixture medium of $\text{NH}_4\text{OH}/\text{H}_2\text{O}_2/\text{H}_2\text{O}$ is a powerful oxidizing agent that reacts violently with organic compounds; it should be handled with extreme care.) The electrodes were constructed by a 450-nm-thick Au layer deposited on a seed layer of 50-nm-thickness Ti. To avoid the interference of a high electric field to EC detection, one decoupling-ground electrode (200 μm in width) as the cathode of CE electric field was positioned in front of the three-electrode electrochemical system, which in turn consisted of a working electrode (100 μm in width), a reference electrode (100 μm in width), and a counter electrode (200 μm in width), and proceeding from the ground electrode to the counter electrode, the spacing between adjacent electrodes were set at 200, 100, and 200 μm . The electrode layout is shown in Figure 1A. At first, the material of all electrodes was Au metal. For the sake of preventing hydrogen bubble formation and improving the EC determining stability, Pt nanoparticles were electrically deposited on the ground electrode and the reference electrode to be the decoupler and the pseudoreference electrode, separately. The deposition was performed in the CE channel using cyclic voltammetry (CV) (BAS 100 W, Bioanalytical Systems, West Lafayette, IN) repeatedly scanning from -500 to 500 mV and then back to -500 mV versus a Ag/AgCl reference electrode placed in the waste reservoir for 30 cycles with the scan rate of 200 mV/s. The fresh H_2PtCl_6 solution prepared in a Britton–Robinson buffer (pH 4.0) containing 5 mM H_2PtCl_6 with an additive of 0.6 g/L lead acetate (Katayama) was flushed into CE channel after scanning each 10 cycles to supply the material for electrodepo-

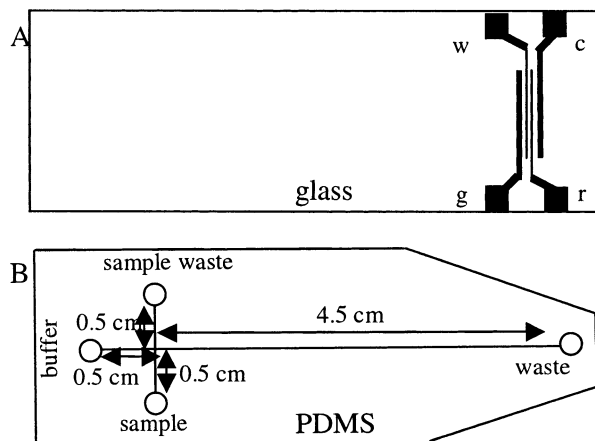


Figure 1. Top view of a microchip used for capillary electrophoresis with electrochemical detection. (A) Electrode layout on glass and (B) the injection and separation channel made from PDMS: (c) counter electrode, (g) ground electrode, (r) reference electrode, and (w) working electrode.

sition.^{36,37} A contact model AFM (P7LS; NT-MDT Co., Zelenograd, Moscow, Russia) was used to examine the surface roughness and area difference of the Au electrode before and after electrodeposition of Pt nanoparticles in air. The surface area corresponding to a data point (pixel) was approximated by doubling the area of the triangle connecting it to two of its nearest neighbors. The resulting rectangular areas corresponding to each data point were added. We used a silicon nitride cantilever (Microlever 06A; Park Scientific Instruments (PSI), Sunnyvale, CA) with a constant force of 0.05 N/m, with an integrated tip 3 μm in height, a 35° half-cone angle, and a curvature radius of 50 nm.

Channel Fabrication and Chip Bonding. The cross-type channel of CE (Figure 1B) was made from PDMS with a 5-cm-long separation channel and a 1-cm-long injection channel with sectional dimensions of 50 μm in height and 30 μm in width. While details of the PDMS channel fabrication matched previously published procedures,^{20–23} the process is briefly described as follows. The cross-type positive relief of thick photoresist, fabricated using standard photolithography, was formed on a silicon wafer to be used as the master to generate PDMS molds for soft lithography. Subsequently, the mixture solution of PDMS monomer with curing agent was cast against the masters at 75 °C for 3 h and then stripped to yield an elastomeric replica. Before bonding the PDMS layer to the glass substrate containing the electrodes, the use of radio frequency O_2 plasma (200 W, 20 s) for the PDMS and glass substrate improved the bonding strength and modified the PDMS surface possessing the hydroxyl group to facilitate the formation of EOF.²⁷ After this step, the four holes as the sample reservoirs were drilled on the end of the channels.

Electrophoresis Procedure. Before any CE test, the channel was filled with running buffer for 30 min. The high voltage was applied by using two high-voltage power supplies (Series. 225, Bertan High-Voltage Corp., Hicksville, NY, and model CZE1000R, Spellman High-Voltage Corp., Plainview, NY) and a high-voltage relay (No. 294-24-C075, Steinecker, Freising, Germany), which was responsible for switching between the sample loading and separa-

(35) Madou, M. *Fundamentals of Microfabrication*; CRC Press: New York, 1997; Chapter 1.

(36) Feltham, A. M.; Spiro, M. *Chem. Rev.* **1971**, *71*, 177–193.

(37) Marrese, C. A. *Anal. Chem.* **1987**, *59*, 217–218.

tion modes. Control of power supply and high-voltage relay was carried out using a GPIB interface and a program the researchers designed using LabVIEW software (National Instruments (NI) Corp., Austin, TX). Pt wires provided electrical contact from the high voltage to the solutions in the reservoirs. The volume of analytes was controlled by applying potentials during the injection and separation modes. To prevent leakage of sample into the separation channel during electromigration injection mode, the applied potentials of the buffer and waste reservoirs were maintained at 75% of the potential applied to the sample reservoir, while the same fraction potential was applied to sample and sample waste reservoirs during separation mode.

Electrochemical Detection. To evaluate the performance of the platinized decoupler, the baseline of detection current recorded from the working electrode was compared with and without the separation electric fields. The baseline offset of detection current was defined as the difference between the EC detection current before and after the application of an electric field. When the decoupler had a better decoupling efficiency, the detection current presented less baseline offset caused from the interference of electrophoretic current. To examine the stability of the platinized pseudoreference electrode during EC detection, 10 mM ferrocyanide filling the whole separation channel was employed to compare the redox reaction before and after the separation field was applied. In the CE-EC experiment, the oxidation current of analytes with a time resolution of 0.5 s was recorded while the detection potential was set at the constant potential of 600 mV versus the platinized pseudoreference electrode. All results of electrochemical detection were recorded, processed, and stored directly on a computer.

RESULTS AND DISCUSSION

CE-EC Microchip Fabrication. A three-electrode electrochemical detector and a decoupler were fabricated in the same chip and integrated with CE channels made of PDMS to produce the CE-EC microchip. This new design of microchip dispensed with the need for both an extra stereopositioner, to align the working electrode and the separation channel, and a separate extrinsic reference electrode or counter electrode for electrochemical detection. The setup of our microchip in CE-EC measurement should be more convenient than previously reported designs and represents the latest design of a replaceable microelectrode.³⁸ Several performance properties of the CE-EC chip will be discussed in the following section.

Evaluation of Decoupler Performance. For a proper evaluation of the decoupler performance, the baseline offset of detection current as a function of different electric fields was recorded through the working electrode at +0.6 V versus a platinized pseudoreference electrode. Readings were further compared with and without an application of the electric field using running buffers of different conductivities, 10 mM MES (pH 6.5, 0.27 mS/cm) and 10 mM PBS (pH 7.4, 1.98 mS/cm). The applied electric field ranged from 50 to 90 V/cm in 10 V/cm steps. From an observation of Figure 2, it can be obviously seen that no matter how the electric field strength varied, or the decoupler material was substituted, the baseline offset of detection current deter-

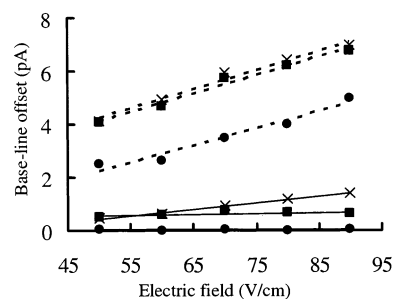


Figure 2. Function of the baseline offset of detection current versus the applied electric field measured in different running buffers and different decoupling conditions. Dashed line, 10 mM PBS (pH 7.4); solid line, 10 mM MES (pH 6.5). Symbols: \times , without decoupler; \blacksquare , with Au decoupler; \bullet , with Pt decoupler.

mined in PBS consistently indicated a higher magnitude than that in MES. This result was attributed to the higher conductivity of PBS to produce the larger electrophoretic current, which could generate more hydrogen and result in the incomplete decoupling of the coupler to interfere with EC detection. In particular, when the strength of an electric field was over 100 V/cm in PBS, hydrogen bubbles that were formed from a dramatic reduction reaction would readily gather at the ground electrode of the high separation electric field and then block the separation channel. In contrast, no matter how high the strength of electric field applied in MES, no obvious bubble formation was observed in this experiment. The use of a decoupler has been shown to decrease the interference from the electric field.^{6,12–17} In this study, a Au or platinized Au electrode was separately used as a decoupler located in front of the EC electrodes. The platinized decoupler, represented by a filled circle in Figure 2, diminished the interference of an electric field much more effectively than the Au metal decoupler, represented by a solid brick. This may be taken to indicate that metals of the Pt group possessed a good ability to absorb and pass hydrogen.¹⁷ In addition, the platinized decoupler has a bigger surface area based on calculation of AFM image, 1.4 μm^2 as shown in Figure 3B, than the raw Au surface, 1.0 μm^2 in Figure 3A, more easily to achieve a decoupling of the electrophoretic current. In particular, because the hydrogen dissipation rate of the platinized decoupler was more than the formation rate in 10 mM MES, the decoupler could relatively completely isolate the electrophoretic current from the EC detection. The baseline offset of detection current could be decreased to the lowest value of ~ 0.05 pA. Furthermore, the peak-to-peak background noise (< 0.7 pA) was obviously smaller than other associated literature being with decoupler.^{6,12–16} It was mainly attributed to apply a smaller electric field for the CE separation and to have a good decoupler. Therefore, all CE efficiency tests were performed in MES with a platinized decoupler to obtain the smallest interference from an electric field.

Stability of the Pt Pseudoreference Electrode. In current whole CE-EC microchips, the reference electrode and counter electrode are externally inserted into the channel outlet reservoir to offer a stable reference potential.^{12,25,26,28,38} In this study, the reference electrode and counter electrode were simultaneously miniaturized and integrated on the same microchip. The platinized Au electrode was used as the pseudoreference electrode. Its performing principle follows that of the hydrogen reference electrode due to the electrocatalyst properties of Pt and its high

(38) Zeng, Y.; Chen, H.; Pang, D. W.; Wang, Z. L.; Cheng, J. K. *Anal. Chem.* **2002** *74*, 2441–2445.

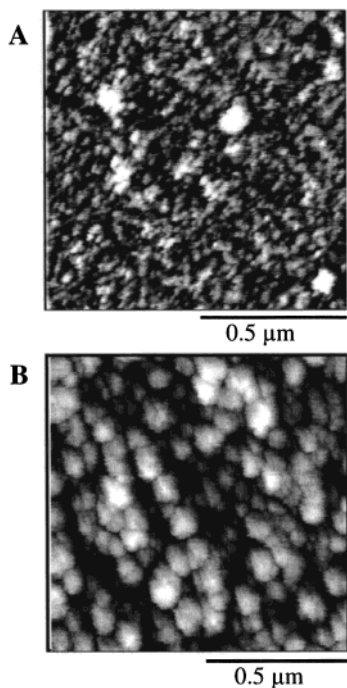


Figure 3. Surface topography of AFM image of Au electrode before (A) and after (B) the platinized electrodeposition. Both scan areas are $1 \times 1 \mu\text{m}^2$.

surface area.^{36,37} CVs of 10 mM ferrocyanide in 10 mM MES (pH 6.5) is shown in Figure 4. This CV behavior was used to determine the stability of the miniaturized EC detector before and after applying the electric field. The redox reaction of ferrocyanide in the microchannel without applying an electric field could be clearly obtained, as shown by the dashed line of Figure 4A. The result indicated that the platinized pseudoreference electrode could offer a stable potential for the working electrode in a confined channel having a stable pH environment. The larger redox peak and high half-wave potential could result from the ohmic potential drop (iR drop) between the working and reference electrodes and the high resistance of the running buffer in a small channel. The CV of ferrocyanide with the application of an electric field and with simultaneous decoupler activation, represented by the solid line of Figure 4A, had the same redox behavior as the previously described CV without application of an electric field. The result was attributed to the good performance of the platinized decoupler in completely decoupling the interference of the CE electric field from EC detection, because the applied CE voltage would cause the shift in half-wave potential of redox species.⁹ The CV in Figure 4B shows that there is no obvious shift through time in the redox potential. Therefore, the miniaturized reference electrode in this CE-EC microchip was demonstrated to be suitable for EC detection.

Efficiency and Lifetime of the CE-EC Microchip. Figure 5 exhibits the influence of strength of an electric field on the EC detection of 1 mM dopamine. The relatively low noise (<0.7 pA) in the background current implied an effective decoupling from the separation electric field through the platinized decoupler. As expected, the migration time decreased with the increase of the separation electric field. The maximum peak current of an oxidative reaction appeared at 75 V/cm. However, the highest number of theoretical plates, $N = 5.54(t_R/W_{0.5})^{2.39}$ was ~ 4800 at

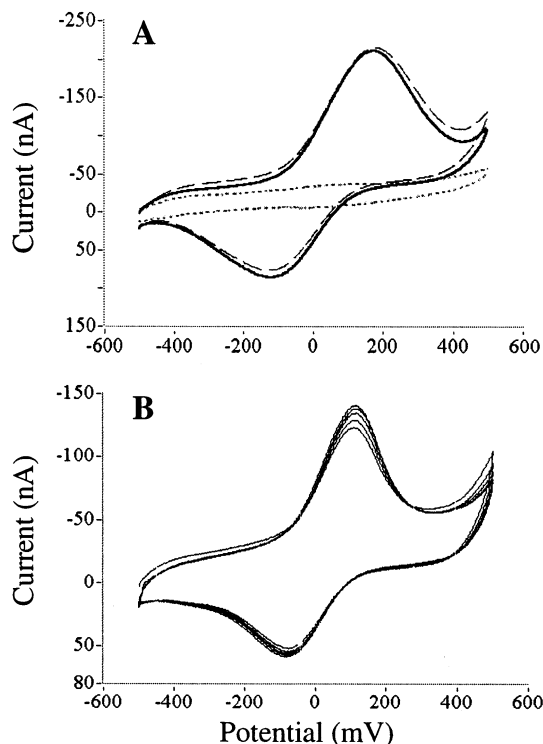


Figure 4. Cyclic voltammograms of 10 mM ferrocyanide prepared in 10 mM MES measured in the separation channel of the CE-EC chip with a scanning rate of 200 mV/s. Working, reference, and counter electrodes are Au, platinized Au, and Au, respectively. (A) Redox reaction with platinized Au decoupler in interference of an electric field (60 V/cm): dotted line, dashed line, and solid line represent the background in MES, without an electric field applied, and with electric field and decoupler connection, respectively. (B) Ferrocyanide was tested for five cycles with a decoupler and electric field application.

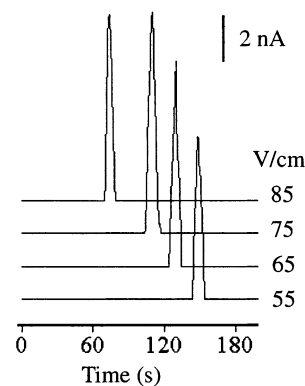


Figure 5. Electropherograms of 1 mM dopamine in 10 mM MES (pH 6.5) performed in different separation strengths of applied electric fields. From top to bottom, the strength of the electric field decreases from 85 to 55 V/cm with a step of 10 V/cm. Amperometric detection at +0.6 V vs platinized pseudoreference electrode.

65 V/cm. Therefore, the applied electric field for linear range measurement of analytes concentration was set at 65–75 V/cm. Presently, the limit of detection of dopamine was $0.125 \mu\text{M}$, which can be routinely observed in MES in the separation field of 65 V/cm with a S/N of ~ 4 , as shown in Figure 6A. The responses for dopamine to different concentrations were found to be linear

(39) Weston, A.; Brown, P. R. *HPLC and CE fundamentals and applications*; Academic Press: London, 1997; Chapter 1.

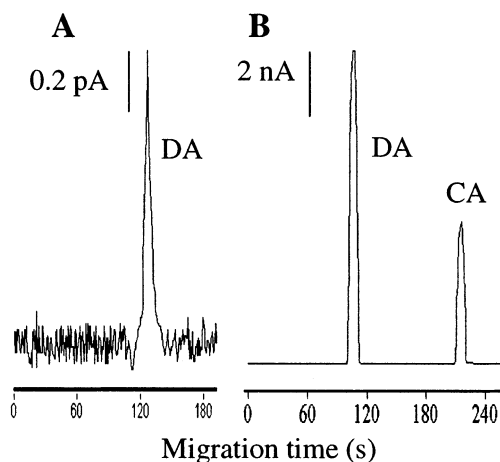


Figure 6. Electropherograms of (A) 0.125 μM dopamine (DA) in the electric field of 65 V/cm and (B) 1 mM dopamine and 1 mM catechol (CA) in the electric field of 75 V/cm. Conditions: amperometric detection at +0.6 V vs platinized pseudoreference electrode in 10 mM MES (pH 6.5).

between 0.25 and 50 μM with a correlation coefficient of 0.9974 and a sensitivity of 11.76 pA/ μM . In most electrophoresis separation, the numbers of theoretical plates were generally less than 5000. Such low separation efficiency could be ascribed to the unstable property of O_2 -plasma-treated PDMS. Duffy et al. pointed out the decay of the hydrophilic layer of the PDMS surface, resulting in the decline of EOF strength, when exposed to the atmosphere.²⁷ Because of some limitations of our present fabrication equipment, the O_2 -plasma-treated PDMS was not immediately sealed with glass substrate. If the shortcoming can be overcome by means of immediate bonding, the number of theoretical plates will be greatly improved. In addition, the negative charge molecule, 1 mM ferrocyanide, was used to demonstrate the EOF existence in this O_2 -plasma-treated PDMS-glass CE chip because it can be regularly detected with a migration time of 240 s at 65 V/cm. Figure 6B demonstrates that the CE-EC microchip had a good separation performance in clearly separating the mixture of 1 mM dopamine and 1 mM catechol.

The other concern is the lifetime of the decoupler and the fully integrated EC detection system. Figure 7 shows the successive electrophoretic measurement of 0.5 μM dopamine in the same microchip. The background noise from the first time to the fifteenth time, being 0.05 to 0.96 pA, had gradually increased. Especially, after the eleventh measurement the background increased significantly. The increase of background noise indicated that the decoupling efficiency of platinized decoupler decreased with the increase of measurement times. The result was attributed to the pollution of decoupler surface, excitation analyte absorbance. When the pollutant covered the most decoupler surface, the decoupling efficiency would decrease and let electrophoretic current affect the EC detection, for example, the increase of background noise and shifted redox potential.^{7,9} Similarly, both the working electrode and pseudoreference electrode could also be polluted by analyte. After the eleventh measurement, the peak height value of the EC current decreased by more than one-tenth. The result suggested that the overpotential increase and surface area decrease of the working electrode arose from electrode pollution and the interference of the

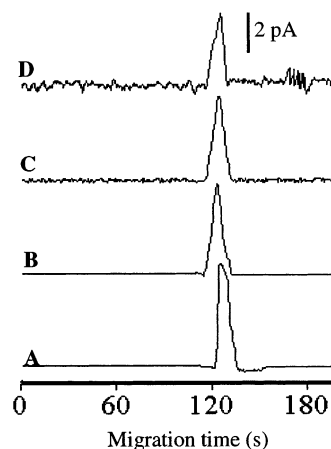


Figure 7. Electropherograms of successively measurement of 0.5 μM dopamine in the same capillary electrophoresis microchip with the separation electric field of 65 V/cm. (A–D) were the first, the fifth, the tenth, and the fifteenth measurement, respectively. Other EC conditions are the same as for Figure 6.

electrophoretic current would result in less oxidation of dopamine at the same oxidative potential (+0.6 V). Therefore, the ideal lifetime of the CE-EC microchip is that the microchip could be allowed to be repeatedly measured at least eleven times and still maintains the same peak height at the same analyte concentration and redox potential.

CONCLUSIONS

This paper first represents the use of a microfabrication technique to simultaneously integrate a three-electrode electrochemical detector and decoupler with an O_2 -plasma-treated PDMS layer containing a CE channel to complete a CE-EC microchip. Experimentally, the results of baseline offset of EC background current, CV of ferrocyanide, and analyte electropherogram demonstrated that the platinized decoupler had sufficient capacity to isolate the interference of the separation electric field in 10 mM MES. It also indicated that a platinized pseudoreference electrode could offer a stable potential when amperometric detection was performed. Unlike joint connected decouplers made of porous joints or polymeric membrane, the platinized decoupler was relatively robust and would not cause any analyte leakage. In addition, the EC detection was so convenient for it was not necessary to apply the positioner to offer the reproducibility of channel-electrode alignment. Such a novel approach should advance the miniaturization and commercialized realization of a CE-EC microchip based on the concept of lab-on-a-chip.

ACKNOWLEDGMENT

The authors thank the National Science Council (Grant NSC89-2218-E-006-069) for financial support, and the Southern Region MEMS Research Center of the National Science Council of the Republic China for facilities to support MEMS fabrication.

Received for review July 2, 2002. Accepted December 18, 2002.

AC025912T